Available online at www.sciencedirect.com
ScienceDirect
Catalysis Today 127 (2007) 44–53
CATALYSIS TODAY
www.elsevier.com/locate/cattod

# Study of the accessibility effect on the irreversible deactivation of FCC catalysts from contaminant feed metals

A.C. Psarras [a,b,*], E.F. Iliopoulou [a], L. Nalbandian [a], A.A. Lappas [a], C. Pouwels [c]

[a] *Laboratory of Environmental Fuels and Hydrocarbons (LEFH), Chemical Process Engineering Research Institute/Center for Research and Technology Hellas, CPERI/CERTH, 6th km Harilaou-Thermi Road, P.O. Box 361, Thermi, 57001 Thessaloniki, Greece*
[b] *Department of Chemical Engineering, Aristotle University of Thessaloniki, P.O. Box 1517, University City, 54006 Thessaloniki, Greece*
[c] *Albemarle Catalysts Company BV, Stationsplein 4, P.O. Box 103, 3800 AC Amersfoort, The Netherlands*

Available online 2 July 2007

**Abstract**

Two commercial FCC catalysts were investigated to explore the effect of their different accessibility on the catalyst activity, selectivity and deactivation due to deleterious feed metals (V and Ni). Feed metal Fe was not included in the present study. E-Cats (equilibrium samples from a commercial FCC unit) of both FCC catalysts and the corresponding laboratory-deactivated samples (applying the cyclic deactivation (CD) and the cyclic propylene steaming (CPS) methods) were thoroughly studied. Extensive characterization (XRD, $N_2$ physisorption, measurement of Akzo Accessibility Index (AAI), SEM-EDS analysis) of all samples was realized to investigate variations in their crucial properties due to metal deposition. Comparison of E-Cats, CD and CPS samples revealed a very different nickel deposition profile over the CPS samples. In all cases, V was homogenously distributed throughout the particle, as expected due to its mobility. Ni–Al mixed phases, observed on the E-Cat samples, were probably formed during ageing and are expected to be inactive. The absence of such phases on the laboratory-deactivated samples can be attributed both to the inability of the two deactivation methods to simulate metal ageing during commercial utilization of the FCC catalyst and the absence of Fe incorporation during laboratory deactivation. All catalytic samples (E-Cats and artificially deactivated FCC catalysts) were evaluated in the laboratory using two bench-scale Microactivity Test (MAT) units of different reactor configuration: fixed-bed (SCT-MAT unit) and fluid-bed (AUTOMAT unit). Similar ranking of the catalysts is achieved when using both units. However, AUTOMAT unit seems to provide a clearer diversification of catalysts with different accessibility. Both laboratory deactivation methods seem to be rather inefficient in simulating the real deactivation, since they are always exaggerating metal effects.


*Keywords:* FCC catalyst; Accessibility; Deactivation; Deleterious feed metals

## 1. Introduction

The recent oil crisis has caused a drastic change in the demand pattern for products of petroleum refining. The demand for heavier fractions has steadily decreased, while that for gasoline, diesel and lighter hydrocarbon fractions is continuously increasing. The solution to that change is to crack more and more of resid fractions into lighter distillates. However, the residual cracking poses numerous problems for the oil companies and the catalyst manufacturers. The increasing portion of large molecules containing hetero-atoms and metal contaminants in fractions of increasing boiling point mainly accounts for the difficulties in processing heavy oils [1]. Residual oils contain a lot of contaminant metals, such as V, Ni and Fe that cause severe deactivation of catalysts. Under the Residuum Fluid Catalytic Cracking (RFCC) operating conditions, almost 100% of these metal contaminants deposits on the catalyst surface [2]. Consequently, problems associated with decreased catalyst stability, activity and selectivity are becoming more often and more serious, demanding new FCC catalyst technologies.

There are several ways of classifying the various forms of catalyst deactivation. First of all, poisoning of the FCC catalyst may be reversible or irreversible. The first case is mainly related with coke, while the latter case is related with deleterious

* Corresponding author at: Laboratory of Environmental Fuels and Hydrocarbons (LEFH), Chemical Process Engineering Research Institute/Center for Research and Technology Hellas, CPERI/CERTH, 6th km Harilaou-Thermi Road, P.O. Box 361, Thermi, 57001 Thessaloniki, Greece.
Tel.: +30 2310 498351; fax: +30 2310 498380.
*E-mail address:* psarras@cperi.certh.gr (A.C. Psarras).

0920-5861/$ – see front matter © 2007 Elsevier B.V. All rights reserved.
doi:10.1016/j.cattod.2007.05.021

metals from the FCC feed. Both of them (coke and metals) are deposited on the catalyst during cracking. During FCC operation basic and polar molecules, e.g. nitrogen compounds, reversibly act as poisons, as they are readily adsorbed on the catalyst acidic sites, leading to an instantaneous, but temporary deactivation. Polycyclic aromatics and other organic and non-strippable molecules are also considered as reversible catalyst poisons, as they behave like coke. The coke deactivation severity depends significantly on the nature of coke, its structure and morphology and finally its exact location on the catalyst surface. Catalyst age distribution is also considered as a major, influential factor on catalyst deactivation [3].

On the other hand, irreversible catalyst poisons start influencing the catalyst, even during its first introduction in the riser reactor, but are not removed during the stripping and/or regeneration stages. Metals present in the feed such as vanadium, nickel, iron and copper or other (e.g. alkali components) are examples of irreversible poisons for FCC catalysts [3]. Ni and V, the mostly recognized deleterious metals for FCC catalysts, are well known dehydrogenation catalysts. Ni is considered to have approximately three to four times higher dehydrogenation activity than V, but V additionally destroys the crystallinity of the zeolitic component of the FCC catalyst [4–9].

Besides metals, hydrothermal deactivation is also irreversible and includes combined action of water and high temperatures. Water, existing as steam at high temperatures, causes the hydrolysis and collapse of the zeolite Al–O–Si bonds. This leads to zeolite dealumination, which typically destroys its surface area, creates mesoporosity and leaves Al as extra-framework species, located either within the existing micropores or forming deposits on the exterior surface of the zeolite crystallites. Migration of extra-framework alumina species from the interior of the zeolite structure depends strongly on the temperature and the steam partial pressure. The lower content of framework Al in dealuminated zeolites is basically reflected to a lower average unit cell size (UCS), as Al–O bond length is bigger than Si–O bond length and Si is replacing Al for stabilization of the structure [10,11].

As a result of the coke and heavy metals deposition on the FCC catalyst, fouling and pore mouth plugging phenomena can be observed. Fouling can cause large differences in catalyst selectivity, as a result of changes in pore architecture [3]. Pore plugging gives rise to issues of accessibility and heterogeneity of the porous catalyst matrix. Both properties are influenced by the degree of interconnectivity of the pore network. Definition of accessibility is stated as ‘‘the ability of the catalyst to have active sites accessible to large molecular structures, which are supposed to interact with these sites within a certain time limitation set by the catalytic process’’ [12,13].

Due to the complexity of the deactivation mechanisms, the prediction of the commercial catalysts’ performance is one of the most important research activities in the oil refining industry [14]. As a result, one of the biggest challenges in FCC research field is to first simulate how the fluid cracking catalyst is deactivated in a commercial FCC unit and then evaluate its performance in laboratory-scale testing [15]. It should be underlined here that selecting the proper catalyst deactivation method is just as important as the testing itself. Thus, there is a need for the development of a realistic deactivation technique that would simulate in the laboratory the deactivation of catalysts in a commercial FCC unit, under the combined action of metals, steam, temperature, thermal shock, etc. [16].

In our earlier work [17], we investigated the effects of two metal poisons (Ni, V) in an FCC pilot plant and performed a comparison study of the metal distribution over catalysts aged in the FCC pilot plant, a cyclic deactivation unit (CDU) or an industrial FCC unit. Correlation of the process performance with the structural properties of FCC catalysts during coke formation was also attempted [18].

The scope of the present study was to investigate the capability of the laboratory (CD and CPS) deactivation methods to simulate commercial deactivation of the FCC catalysts affecting both their performance and their properties. Besides effects of contaminant metals (Ni, V) on the catalyst structure, the present work focuses on the effect of accessibility differences on the performance and deactivation of the FCC catalysts. In parallel, laboratory methods evaluating FCC catalysts’ performance (Microactivity Test units of different design) were also explored.

## 2. Experimental

### 2.1. Materials

Two commercial FCC catalysts were supplied by Albemarle Catalysts Company and fully evaluated in two bench-scale Microactivity Test (MAT) units. The main difference between these two catalysts is their accessibility, a term defined in previous sections. The FCC catalysts with the high and low accessibility will be referred as HA-Cat and LA-Cat, respectively. The HA-Cat and the LA-Cat contained 14,200 and 10,500 ppmw of rare earths, respectively. Both fresh and equilibrium samples were received and tested. Equilibrium samples are catalysts used and deactivated in a commercial FCC unit and will be referred herein as E-Cats. Fresh catalytic samples were also artificially deactivated in our laboratory applying the cyclic deactivation (CD) and the cyclic propylene steaming (CPS) methods. The detailed laboratory deactivation procedures are given in a following section. A commercial FCC residual feedstock was used in all evaluation experiments (S.G.: 0.9169; density (60 °C): 0.8856 g/cm$^3$; density (15.5 °C): 0.916 g/cm$^3$; S: 0.6094 wt.%; distillation data {wt.%, °C}: {10, 393.5}, {20, 414.5}, {30, 429.3}, {40, 442}, {50, 454.4}, {60, 467.8}, {70, 483.1}, {80, 500.1}, {90, 524.2} and {FBP, 551.6}).

### 2.2. Characterization

All catalytic samples, fresh, commercially or artificially deactivated, were submitted to a standard series of characterization techniques. More significantly, the specific surface area, the micropore volume and the pore size distribution of the catalysts was determined by nitrogen adsorption (BET

Table 1
Properties of the fresh, E-Cat and laboratory-deactivated LA-Cat FCC catalyst

| Catalytic sample | Fresh-LA-Cat | CPS-LA-Cat | CDU-LA-Cat | E-Cat-LA-Cat |
|---|---|---|---|---|
| Total surface area ($m^2$/g) | 268.4 | 181.2 | 168.1 | 131.9 |
| Zeolite surface area ($m^2$/g) | 204.7 | 139.4 | 126.6 | 100.8 |
| Matrix surface area ($m^2$/g) | 63.7 | 41.7 | 41.4 | 31.1 |
| Zeolite/matrix | 3.2 | 3.3 | 3.1 | 3.2 |
| Unit cell size (Å) | 24.61 | 24.29 | 24.29 | 24.27 |
| Ni (ppmw) | 17 | 3126 | 2970 | 5995 |
| V (ppmw) | 33 | 774 | 737 | 1357 |
| Fe (ppmw) | 2045 | Not measured | Not measured | 5510 |

Table 2
Properties of the fresh, E-Cat and laboratory-deactivated HA-Cat FCC catalyst

| Catalytic sample | Fresh-HA-Cat | CPS-HA-Cat | CDU-HA-Cat | E-Cat-HA-Cat |
|---|---|---|---|---|
| Total surface area ($m^2$/g) | 202.2 | 140.2 | 140.6 | 111.5 |
| Zeolite surface area ($m^2$/g) | 93.3 | 57.7 | 64.3 | 64.9 |
| Matrix surface area ($m^2$/g) | 108.9 | 82.5 | 76.3 | 46.7 |
| Zeolite/matrix | 0.9 | 0.7 | 0.8 | 1.4 |
| Unit cell size (Å) | 24.68 | 24.42 | 24.44 | 24.36 |
| Ni (ppmw) | 26 | 3270 | 2553 | 5979 |
| V (ppmw) | 36 | 637 | 629 | 1068 |
| Fe (ppmw) | 2418 | Not measured | Not measured | 6629 |

method), using an Autosorb-1 Quantachrome flow apparatus. The crystalline structure and especially the unit cell size of the catalysts was studied recording powder X-ray diffraction patterns in a Siemens D500 diffractometer with auto-divergent slit and graphite monochromator, using Cu Kα radiation. The bulk concentrations of deleterious metals and other elements were measured with ICP/AES analysis, carried out in a Plasma 400 (Perkin-Elmer) spectrometer, equipped with Ceta-c6000AT+ ultrasonic nebulizer. All characterization results for all catalytic samples are given in Tables 1 and 2.

Akzo Accessibility Index (AAI) of all catalytic samples was measured by Albemarle using the standard Albemarle/Akzo protocol and the corresponding data are included in Table 3. AAI is measured applying a rapid screening test, mainly based on liquid-phase diffusion of large organic molecules into the catalyst. No reaction is involved and the test only determines the catalysts' initial mass transfer characteristics. The test includes placing the catalyst in a solution of dissolved petroleum and monitoring the solution's penetration using an on line UV spectrometer. The AAI is a relative measure of the penetration rate [16,19]. More detailed description of the technique is constricted due to confidentiallity reasons.

Table 3
AAI of all the catalytic samples

| Sample | AAI |
|---|---|
| Fresh-LA-Cat | 4.3 |
| Fresh-HA-Cat | 15.5 |
| E-Cat-LA-Cat | 3.1 |
| E-Cat-HA-Cat | 5.0 |
| CPS-LA-Cat | 9.7 |
| CPS-HA-Cat | 21.3 |
| CDU-LA-Cat | Not measured |
| CDU-HA-Cat | 18.6 |

The morphological characteristics of the catalyst samples were examined by scanning electron microscopy (SEM, JEOL 6300) equipped with X-ray microanalysis (OXFORD ISIS 2000). Scanning electron microscope magnification ability was from 10 up to 300,000. Elemental microanalysis and mapping of surfaces was achieved using the X-ray energy dispersive spectroscopy (EDS) system. SEM images were obtained either from the outer part of catalytic particles or from the particle cross-sections. In order to examine the interior of the very small particles, they were embedded in epoxy resin, ground and polished up to 1 μm. Local elemental composition measurements as well as elemental maps were obtained only from the flat cross-section images.

### 2.3. Bench-scale units for the laboratory deactivation of FCC catalysts

The cyclic deactivation (CD) method and the cyclic propylene steaming (CPS) method were used for the artificial deactivation of the fresh samples in the laboratory. The complete CD-run consists of 54 cycles, while each cycle includes a cracking, stripping and regeneration step. Prior to CD, all samples are initially submitted to a calcination pre-treatment in a 40% $O_2$–60% $N_2$ flow, for 2 h. A gas oil, spiked with nickel and vanadium naphthenates is used as the feed in the CD unit. Cracking is carried out at 500 °C, under $N_2$ flow and using a catalyst to oil ratio equal to 10. Regeneration is carried out at 788 °C in gas flow (40% $O_2$–60% $N_2$). After 47 cycles, a small portion of the catalyst is replaced and after 51

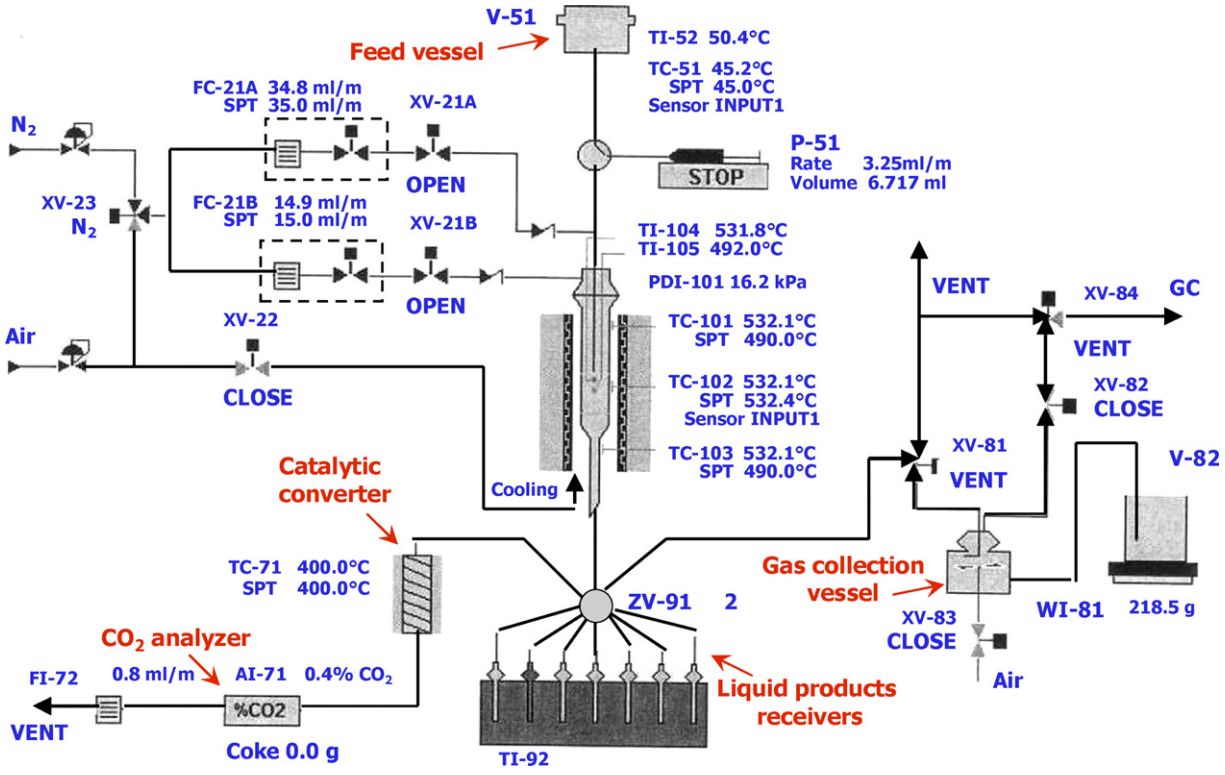


Fig. 1. AUTOMAT experimental unit.

cycles a small amount of catalyst is added in order to achieve some FCC catalyst age distribution.

In the CPS method, V and Ni are initially deposited on the fresh FCC catalytic samples by wet impregnation, followed by deactivation in a series of reduction–oxidation cycles [20]. According to the standard CPS protocol, the samples were at first submitted to a calcination pre-treatment in air flow at 205 °C for 1 h and then at 595 °C for 3 h. Then, the wet impregnation was carried out using solutions of nickel and vanadyl naphthenates in toluene [20]. The specific solutions were selected because they mimic metal species in the feed, reported to exist mainly as organic complexes with porphyrins [21]. The metal concentration target in the artificially deactivated samples was the 50% of the metal content of the corresponding E-Cats. The solvent was totally removed by heating the mixture at 100–110 °C in a rotary evaporator. After that, the sample was submitted to a calcination treatment in air flow at 205 °C for 1 h and then at 595 °C for 3 h in order to decompose the naphthenates. Finally, the catalysts were deactivated via a series of reduction–oxidation cycles. It should be underlined that the procedure is starting with a stripping step and finishing with a reducing step. These cycles are repeated up to 30 times to give a total run time of 20 h.

### 2.4. Bench-scale units for the evaluation of FCC catalysts

All evaluation studies were carried out in two bench-scale microactivity units: a short contact time fixed-bed Micro-activity Test unit (SCT-MAT) and a fully automated, fluid-bed MAT unit, referred herein as AUTOMAT unit. Details on the design and the experimental conditions of the SCT-MAT unit can be found elsewhere [22]. Besides reactor configuration, the major difference between SCT-MAT and AUTOMAT units is that the latter also provides the possibility of in situ regeneration at 650 °C. The AUTOMAT unit is fully automated, limiting the effect of human factor on the experimental data. A schematic diagram of the AUTOMAT unit is given in Fig. 1. Cracking is realized at 560 °C in both units, while reaction time is 12 and 75 s in the SCT-MAT and the AUTOMAT unit, respectively. Finally evaluation of catalysts is realized over a series of cat-to-oil ratios. This is achieved in the SCT-MAT unit by altering the mass of catalyst and in the AUTOMAT unit by altering the mass of feed.

Analysis of gas products and coke measurement is performed on line, after each run, while liquid products should be collected and analyzed. Gas products are analyzed by a gas chromatograph (HP-6890) equipped with two thermal conductivity detectors (TCD). Measurement of coke was realized as follows: the regeneration gases passed through a catalytic converter ($V_2O_5$) in order to convert any CO to $CO_2$ and then were led to a non-dispersive infrared analyzer (NDIR) (LIRA MODEL 3250) continuously measuring the $CO_2$. Integration of the curves of $CO_2$ emissions versus regeneration time provided calculation of the total amount of coke. Finally, liquid products were analyzed with a gas chromatograph (GC-260) equipped with a flame ionization detector (FID) and a column able to fractionate the sample by the boiling point.

## 3. Results and discussion

### 3.1. Characterization studies

All samples were submitted to a series of standard characterization techniques, summarized in Tables 1–3. We should mention that since we did not incorporate iron impregnation during the application of laboratory deactivation methods we did not measure Fe concentration on the laboratory-deactivated samples. As obvious from Tables 1 and 2 neither CPS nor CDU method achieved to simulate the characteristics of the equilibrium samples. Furthermore, the deactivation methods were found less accurate for the accessibility simulation on the high accessible catalyst. The results of the pore size distribution (cumulative pore volume $d < 130$ Å $\{cm^3/g\}$—CPS-HA: 0.134, CPS-LA: 0.049, CDU-HA: 0.136, CDU-LA: 0.048, E-Cat-HA: 0.073, E-Cat-LA: 0.036, Fresh-HA: 0.145, Fresh-LA: 0.065) are consistent to the AAI measurement, as the laboratory-deactivated samples were found to be far more accessible than the corresponding E-Cats and the deviation on the high accessible catalyst was greater. On the other hand, as obvious from Table 3, the laboratory-deactivated samples were found more accessible than the corresponding fresh samples, as expected from previous studies [16]. The paradox of the higher accessibility of the lab-deactivated samples is probably related with changes in the structure and tortuosity of the catalysts' pores.

Besides standard characterization, all the samples were further explored using the SEM-EDS method. Our scope was to observe the distribution of various elements throughout the catalyst particles, as a result of various deactivation conditions. Investigating variations in metal deposition profiles among equilibrium and laboratory-deactivated samples we could check the ability of the laboratory deactivation techniques to simulate commercial deactivation. E-Cat samples were analyzed first (Fig. 2) in order to obtain the metal distribution images of the real case. As obvious from the corresponding SEM pictures, Fe is deposited on the outer surface of both particles, as expected [23,24], while its concentration in the interior of the catalytic particle is significantly lower. On the contrary V is well distributed all over the particle (not shown here), due to its migration ability [25,26]. Concerning finally Ni species, their majority is deposited on the outer surface (Fig. 2), as expected [27]. However, some local areas of high Ni concentration are also observed in the internal of the particle. It seems that Fe and Ni are deposited deeper in the HA-Cat particle than in the LA-Cat, probably due to its higher accessibility.

In order to investigate the internal locations of nickel enrichment, we performed a point analysis study. Complete elemental analysis is performed at many different points, selected by the user. One can select the points as a function of the distance from the particle edge, or in areas of apparently different composition. The results are presented in Fig. 3. In most cases, we noticed that local areas of Ni enrichment are also areas of Al enrichment. This can be attributed to the formation of Ni–Al mixed phases, like nickel aluminate [27,28], which are probably created during metal ageing.

Following that, we examined the artificially deactivated samples. We should mention that the profile of vanadium distribution was similar on all samples, and homogenously distributed throughout the particle. Over both CPS samples we observed that nickel is evenly distributed throughout the particle (Fig. 4), in contrast with the situation over the commercially deactivated catalytic samples (E-Cats). Such a profile was rather expected due to the metal deposition using the wet impregnation method. In the commercial process the competitive adsorption of Ni with the reactant molecules of the

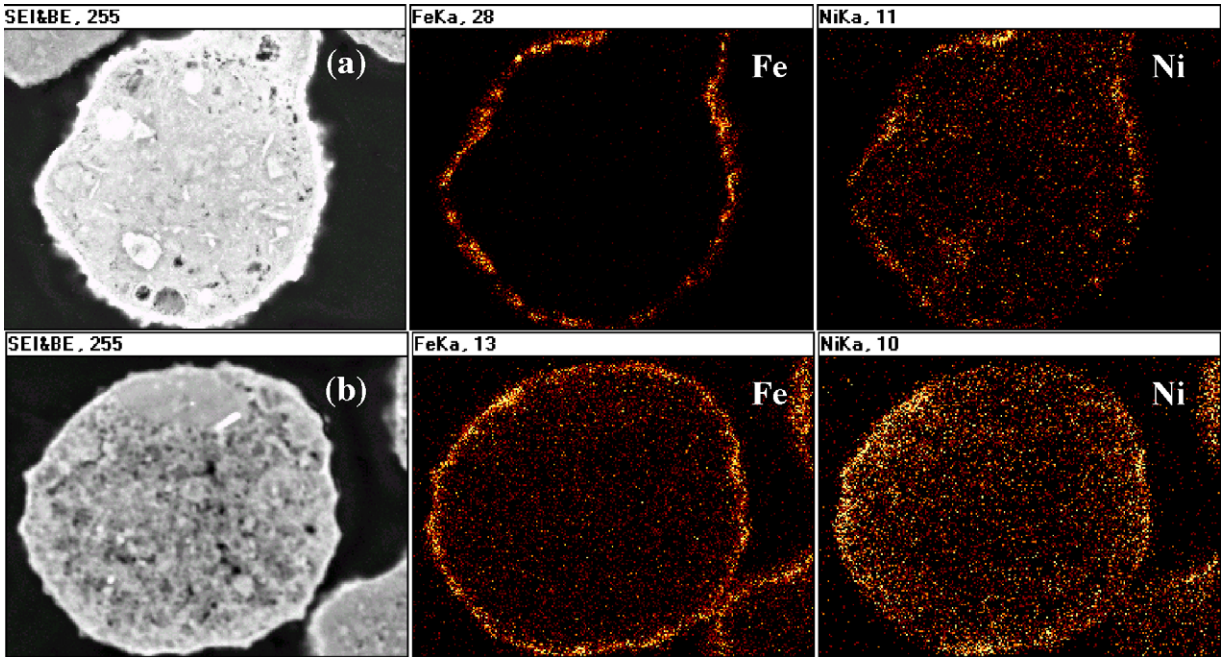


Fig. 2. Element mapping over E-Cat samples: (a) E-Cat-LA (low accessibility) and (b) E-Cat-HA (high accessibility).

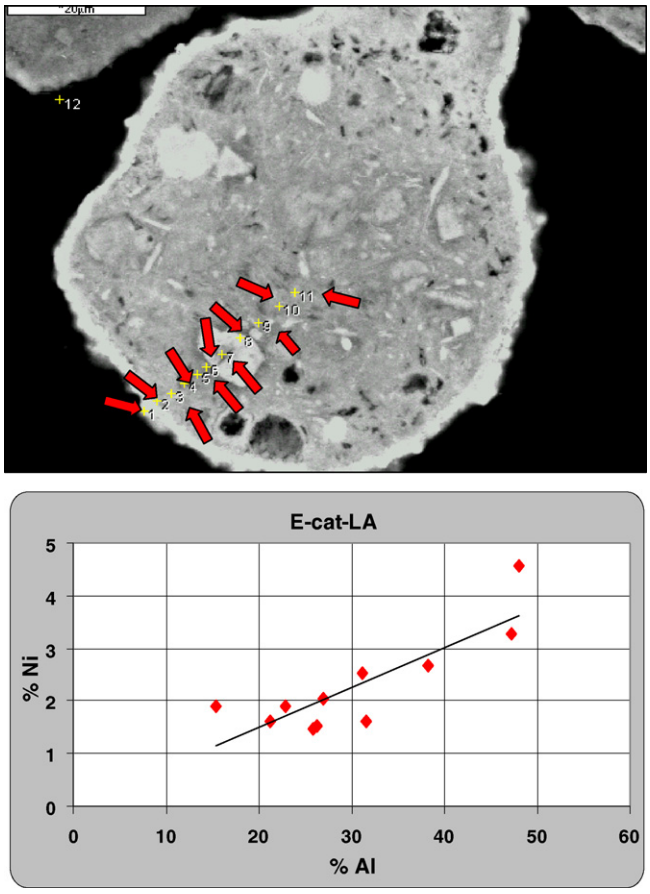


Fig. 3. Ni–Al correlation on the E-Cat-LA (low accessibility) sample.

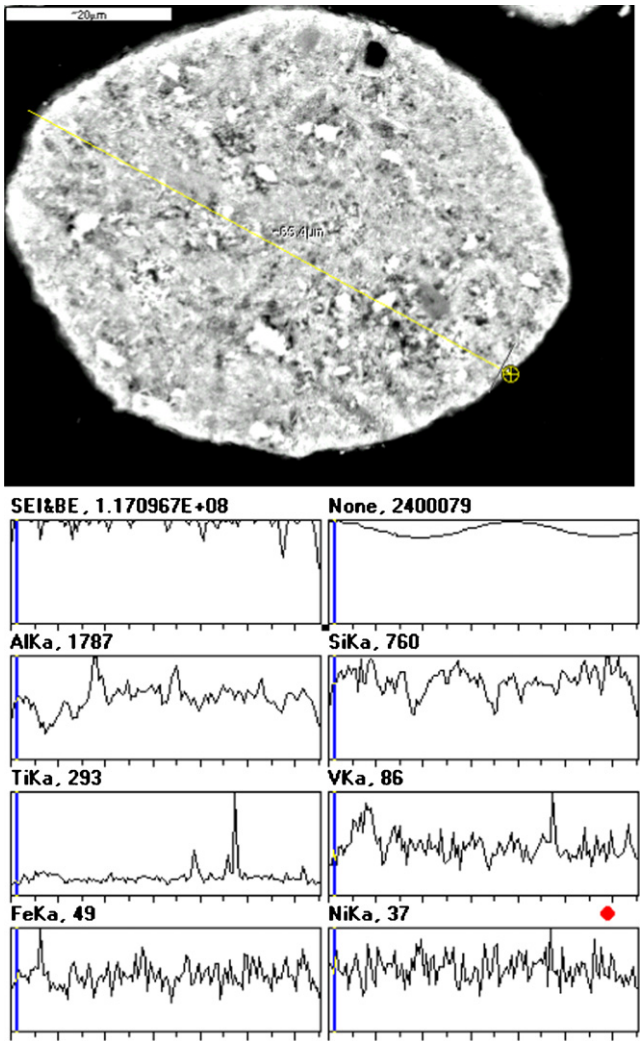


Fig. 4. Linescan over the CPS-HA (high accessibility) sample.

feed could affect the distribution of Ni. The absence of such competitive adsorption during the wet impregnation step of CPS method could count as an extra reason for the different distribution profile of nickel. However, a limited Ni enrichment was interestingly observed on the surface of the LA catalyst (Fig. 5), which may be related to its lower accessibility. Absence of Ni–Al mixed phases on both samples reveals the shortness of the CPS method in simulating commercial deactivation and especially metal ageing.

Finally, the samples deactivated via CD procedure were also investigated by SEM-EDS technique. Both CDU-HA-Cat and CDU-LA-Cat seem to present a more realistic metal distribution. Nickel is concentrated mostly on the surface (Fig. 6), while vanadium seems well distributed all over the particle. Once more no Ni–Al mixed phases were observed on the CDU catalytic samples, indicating that metal ageing is again not satisfactorily achieved.

### 3.2. Equilibrium catalysts' evaluation

Both equilibrium samples were initially tested in order to obtain a base case for the evaluation of catalytic performance, used in the following for the evaluation of the laboratory-deactivated samples. Comparison of the two types of FCC catalyst shall provide useful information concerning the accessibility effect on the catalytic performance. We should clarify that the evaluation of the catalysts was carried out in both microactivity units (SCT-MAT and AUTOMAT) in order to additionally investigate the effect of the reactor configuration on the catalysts' evaluation procedure.

These first series of experiments avouched the fact that both units are accepted for evaluating FCC catalysts. Data on product yields delta between two types of FCC catalysts, at the same conversion level (60%), during evaluation in both MAT units are summarized in Table 4. As obvious from this table, the olefinicities deltas are higher during evaluation in the AUTOMAT unit. Olefinicity is defined as the ratio of the olefins yields to the total hydrocarbon yields (paraffins + olefins) with the same carbon number. Olefinicity can count as an indirect measurement of the secondary hydrogen transfer reactions, which are promoted by a low diffusion rate and thus, strongly related with accessibility. Hydrogen transfer reactions are bimolecular, thus their progress is depending on the acid sites density as well. Despite the fact that E-Cat-HA maintained bigger UCS, indicating that this sample has higher acid sites density and should promote the hydrogen transfer reactions, a higher olefinicity was observed on both units indicating that accessibility had a greater impact on the progress of the hydrogen transfer reactions. It seems that diversification of

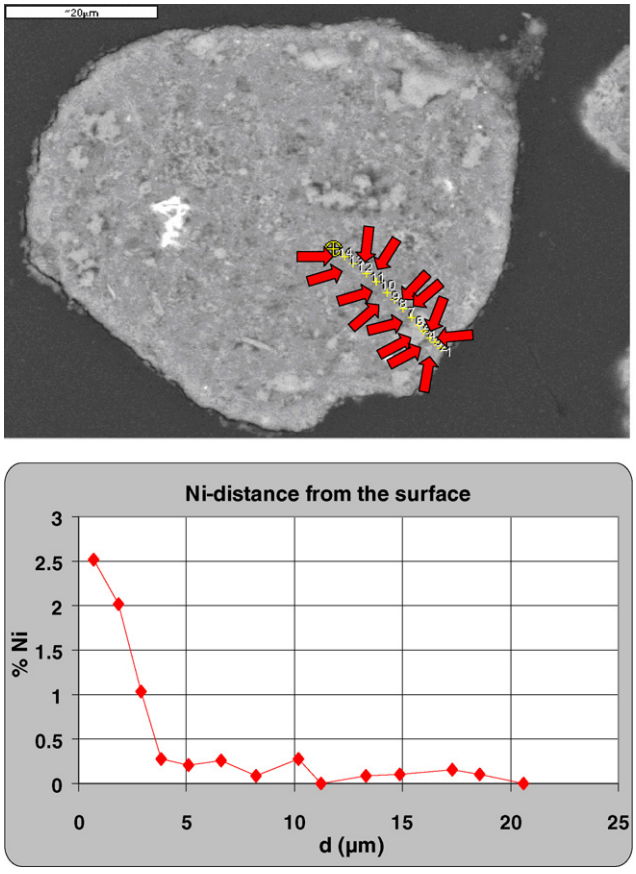


Fig. 5. Ni concentration vs. distance from the surface for the CPS-LA sample (low accessibility catalyst deactivated by CPS).

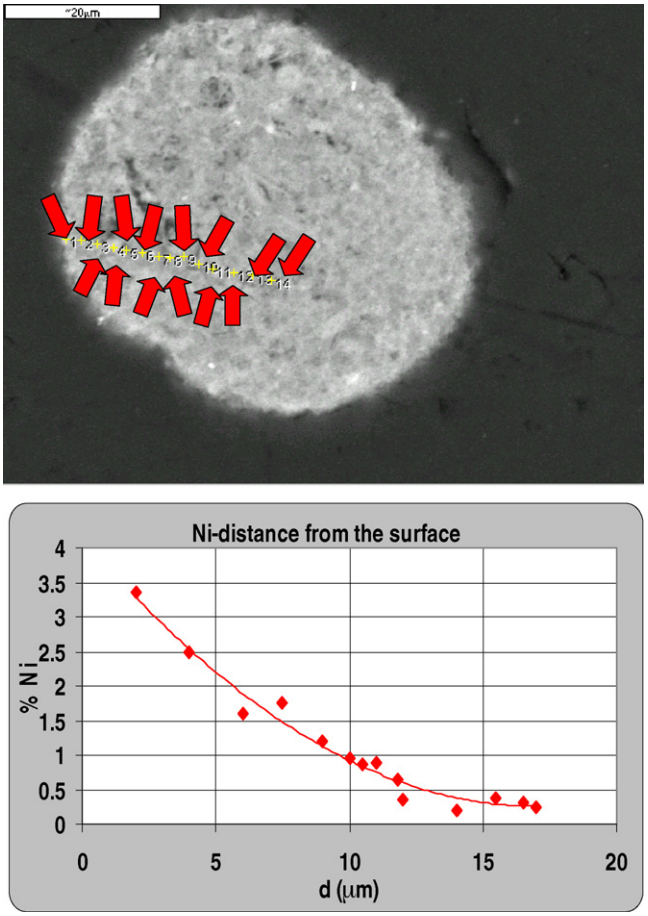


Fig. 6. Ni concentration vs. distance from the surface for the CDU-LA sample (low accessibility catalyst deactivated by CD).

catalysts of different accessibility is evidenced more clearly in the AUTOMAT unit. The lower coke and dry gases deltas in AUTOMAT are also attributed to accessibility differences. In conclusion, a more detailed view of the results supports that AUTOMAT unit provides a slightly better response on accessibility differences.

Activity and selectivity evaluation results are summarized in Tables 5 and 6, concerning utilization of the SCT-MAT or the AUTOMAT unit, respectively. Considering the evaluation of the two E-Cats, the HA-Cat is more active probably because its higher UCS favors cracking. Additionally, larger molecules could more easily reach the active sites and crack on the HA-Cat. As reported in the literature [18], the highly accessible catalysts are able to take advantage of all their active sites, in contrast with the low accessibility catalysts. This is attributed to the fact that the highly accessible catalyst can utilize all of its potential catalytic activity before it is completely deactivated due to pore plugging. On the other hand, when the low accessibility catalyst undergoes complete deactivation, there are still a non-negligible number of active sites remaining unexploited [18]. This possibly explains the higher activity of the HA-Cat in combination to the more active matrix surface area which enhances coke production (Fig. 7). This active matrix also performs a pre-cracking of large molecules resulting in lower HCO yields. This pre-cracking produces species of the diesel range which can possibly re-crack on the

Table 4
Product deltas of the two E-cats during evaluation in SCT-MAT and AUTOMAT units (at 60% conversion)

| | SCT-MAT HA–LA | AUTOMAT HA–LA |
|---|---|---|
| C/O | 0.020 | −0.400 |
| Gasoline | −2.400 | −1.240 |
| Diesel | 1.940 | 1.770 |
| Coke | 1.030 | 0.540 |
| Dry gases | 0.149 | 0.042 |
| Hydrogen | 0.121 | 0.100 |
| Methane | 0.019 | −0.043 |
| Ethane | −0.001 | −0.008 |
| Ethylene | 0.011 | −0.007 |
| Propane | 0.006 | −0.098 |
| Propylene | 0.850 | 0.900 |
| *i*-Butane | 0.000 | −0.260 |
| *n*-Butane | −0.042 | −0.128 |
| 1-Butene | 0.030 | 0.109 |
| *i*-Butene | 0.300 | 0.410 |
| *t*-Butene2 | 0.102 | 0.167 |
| *c*-Butene2 | 0.074 | 0.120 |
| Total $C_3 + C_4$ | 1.300 | 1.220 |
| C3 olefinicity | 0.019 | 0.041 |
| C4 olefinicity | 0.025 | 0.050 |

Table 5
Mass balances of all catalytic samples during evaluation in SCT-MAT unit (at 60% conversion)

| | E-CAT | | CPS | | CDU | |
|---|---|---|---|---|---|---|
| | HA-Cat | LA-Cat | HA-Cat | LA-Cat | HA-Cat | LA-Cat |
| Gasoline | 39.70 | 42.10 | 41.50 | 42.80 | 43.70 | 44.00 |
| Conversion | 60 | 60 | 60 | 60 | 60 | 60 |
| C/O | 3.00 | 2.98 | 2.44 | 2.89 | 1.87 | 2.08 |
| Diesel | 20.75 | 18.81 | 23.00 | 21.80 | 19.00 | 17.70 |
| Coke | 4.02 | 2.99 | 4.60 | 2.90 | 4.30 | 3.00 |
| Dry gases | 1.73 | 1.58 | 2.09 | 1.72 | 1.70 | 1.50 |
| Hydrogen | 0.32 | 0.20 | 0.55 | 0.26 | 0.44 | 0.24 |
| Methane | 0.54 | 0.53 | 0.62 | 0.57 | 0.53 | 0.49 |
| Ethane | 0.38 | 0.38 | 0.46 | 0.44 | 0.35 | 0.33 |
| Ethylene | 0.49 | 0.48 | 0.45 | 0.47 | 0.38 | 0.44 |
| Propane | 0.68 | 0.66 | 0.55 | 0.56 | 0.48 | 0.60 |
| Propylene | 4.85 | 4.00 | 3.53 | 3.67 | 3.05 | 3.35 |
| *i*-Butane | 2.34 | 2.36 | 1.92 | 2.10 | 1.65 | 2.09 |
| *n*-Butane | 0.56 | 0.60 | 0.54 | 0.59 | 0.44 | 0.55 |
| 1-Butene | 1.28 | 1.25 | 1.19 | 1.25 | 1.04 | 1.09 |
| *i*-Butene | 1.99 | 1.69 | 1.57 | 1.66 | 1.39 | 1.40 |
| *t*-Butene2 | 1.62 | 1.52 | 1.41 | 1.49 | 1.20 | 1.29 |
| *c*-Butene2 | 1.25 | 1.18 | 1.01 | 1.16 | 0.95 | 1.02 |
| Total $C_3 + C_4$ | 14.55 | 13.25 | 11.75 | 12.40 | 10.20 | 11.35 |
| C3 olefinicity | 0.88 | 0.86 | 0.87 | 0.86 | 0.87 | 0.85 |
| C4 olefinicity | 0.68 | 0.65 | 0.69 | 0.68 | 0.68 | 0.65 |

zeolite active sites. The coke yields are higher in the Automat unit than in the SCT-MAT unit due to the longer time of reaction. Moreover, it is well known that fluidized bed is always giving more coke as compared with the fixed bed [20,29]. The lower gasoline yield (Tables 5 and 6) of the HA-Cat in both units is attributed to the lower zeolite surface area of the catalyst.

Table 6
Mass balances of all catalytic samples during evaluation in AUTOMAT unit (at 65% conversion)

| | E-CAT | | CPS | | CDU | |
|---|---|---|---|---|---|---|
| | HA-Cat | LA-Cat | HA-Cat | LA-Cat | HA-Cat | LA-Cat |
| Gasoline | 36.45 | 37.96 | 43.80 | 45.95 | 42.49 | 45.10 |
| Conversion | 65 | 65 | 65 | 65 | 65 | 65 |
| C/O | 4.51 | 5.24 | 2.12 | 2.37 | 2.75 | 2.40 |
| Diesel | 22.13 | 19.99 | 21.71 | 20.58 | 21.34 | 19.85 |
| Coke | 8.70 | 8.05 | 9.38 | 5.83 | 10.60 | 7.10 |
| Dry gases | 2.34 | 2.49 | 1.52 | 1.38 | 1.81 | 1.39 |
| Hydrogen | 0.35 | 0.26 | 0.21 | 0.12 | 0.36 | 0.19 |
| Methane | 0.97 | 0.89 | 0.57 | 0.50 | 0.69 | 0.56 |
| Ethane | 0.48 | 0.52 | 0.39 | 0.38 | 0.39 | 0.35 |
| Ethylene | 0.63 | 0.66 | 0.35 | 0.38 | 0.38 | 0.41 |
| Propane | 1.19 | 1.30 | 0.71 | 0.72 | 0.70 | 0.93 |
| Propylene | 5.60 | 4.82 | 2.72 | 3.20 | 2.85 | 3.05 |
| *i*-Butane | 3.26 | 3.56 | 2.10 | 2.44 | 1.98 | 2.61 |
| *n*-Butane | 0.79 | 0.96 | 0.61 | 0.66 | 0.55 | 0.73 |
| 1-Butene | 1.33 | 1.27 | 0.865 | 1.025 | 0.89 | 0.895 |
| *i*-Butene | 1.95 | 1.69 | 1.08 | 1.23 | 1.14 | 1.01 |
| *t*-Butene2 | 1.71 | 1.66 | 1.05 | 1.29 | 1.1 | 1.12 |
| *c*-Butene2 | 1.32 | 1.31 | 0.83 | 1.01 | 0.87 | 0.89 |
| Total $C_3 + C_4$ | 17.13 | 16.60 | 9.95 | 11.60 | 10.10 | 11.00 |
| C3 olefinicity | 0.83 | 0.79 | 0.79 | 0.81 | 0.80 | 0.79 |
| C4 olefinicity | 0.61 | 0.57 | 0.59 | 0.59 | 0.61 | 0.56 |

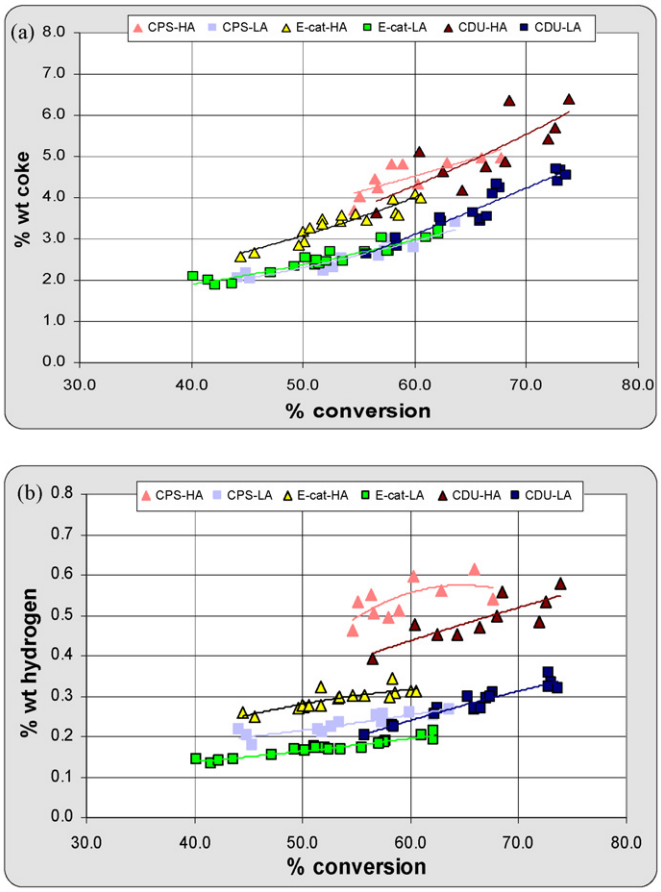


Fig. 7. Coke (a) and hydrogen (b) yield vs. conversion over the E-Cat and laboratory-deactivated catalytic samples in SCT-MAT.

Enhanced hydrogen yields (Fig. 7) were measured during evaluation of the HA-Cat indicating more active poisonous metals. According to the literature, because of the pore blockage, the contaminant metals tend to influence more the catalysts that have high accessibility to active sites [30]. The higher olefinicities provided by the HA-Cat are also strongly related to its higher accessibility, letting the olefins diffuse quickly out of the particle, before they get involved in secondary hydrogen transfer reactions and transform into paraffins.

### 3.3. Laboratory-deactivated catalysts' evaluation

Our next step was to evaluate the artificially deactivated samples, starting from the SCT-MAT unit. Both deactivation methods (CPS and CDU) provided more active catalytic samples, as compared with the E-Cat samples, with higher gasoline yields (Table 5). This was rather expected because of their larger UCSs and total surface areas. Despite the fact that the artificially deactivated samples were prepared to contain only 50% of the E-Cat metal levels (Ni and V), they tend to produce more hydrogen, as presented in Fig. 7a, although coke yields are quite matched (Fig. 7b). This is an indication that deleterious metals in the laboratory-deactivated samples were more active than the metals on the E-Cats. This could be related

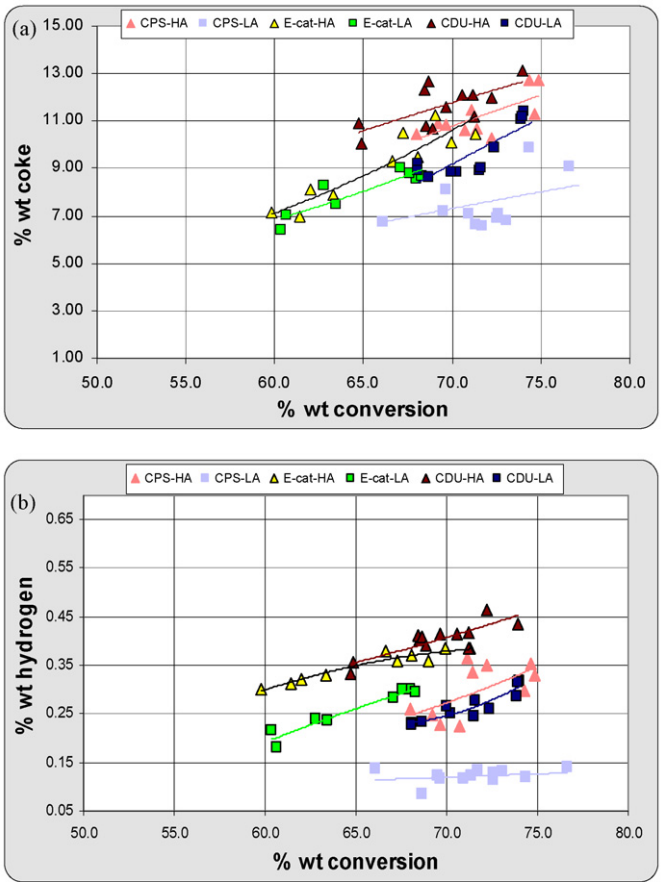


Fig. 8. Coke (a) and hydrogen (b) yield vs. conversion for the E-Cat and laboratory-deactivated samples in AUTOMAT.

with the insufficiency of the laboratory deactivation procedures to simulate metal ageing and a realistic metal deposition. Moreover, the hydrogen yields are enhanced on the CPS-deactivated samples due to extended dehydrogenation reactions. This enhanced dehydrogenation activity, observed on the CPS samples, is probably an effect of higher nickel dispersion. In detail, Lewis acid sites created by nickel are responsible for dehydrogenation reactions, while higher dispersion creates more of these active sites [31]. We suppose that the effect is less visible on LA-Cat due to its lower accessibility, which limits Ni dispersion. Ni oxidation state could be an additional culprit accounting for enhanced hydrogen yields. We should underline here that the last step of the CPS procedure is a reductive one, while as reported in the literature [27]; reduced Ni species are more deleterious, enhancing catalyst deactivation. On the contrary, the contaminant metals are oxidized after the CDU deactivation. Nevertheless we should not forget that oxidized vanadium is more active concerning collapse of the zeolite structure, although it is considered four times less active than nickel concerning dehydrogenation reactions [2,25].

Using the SCT-MAT unit, the accessibility variation between HA-Cat and LA-Cat samples is not so obviously reflected on their olefinicities. This could be related with the fact that both CPS and CDU samples possess a higher accessibility compared with the E-Cat samples (Table 3). It is important to be really careful when considering the effect on olefinicities, as it is a contribution of multiple reactions. So, the highly accessible catalyst should provide limited secondary bimolecular hydrogen transfer reactions, in contrast to oligomerization and cyclization reactions of olefins which are favored in larger pores [32].

The last step of our evaluation studies was to examine the artificially deactivated catalytic samples in the AUTOMAT unit. As obvious from Table 6, the samples from both deactivation methods were found more active than the E-Cats and provided higher gasoline yields. The hydrogen yields (Fig. 8a) of the CD samples are similar to those of the E-Cats, in contrast with the CPS samples that produced less hydrogen. In combination with the SCT-MAT results, we may conclude that the lower hydrogen production is a consequence of secondary hydrogenation reactions. The fact that coke yields of the CPS samples and especially of the LA-Cat sample (Fig. 8b) are also lower during evaluation in AUTOMAT unit supports our conclusion. It is obvious that LA-Cat favored the secondary hydrogenation reactions because of its lower accessibility. As evidenced in Tables 5 and 6, the olefinicities during evaluation in AUTOMAT unit were found quite similar with the olefinicities from the SCT-MAT experiments indicating that the hydrogenation reactions did not significantly affect olefinicities. The lower coke yields support that the hydrogenation reactions mainly affect the coke species.

## 4. Conclusions

Two types of FCC catalysts (of different accessibility), both commercially and artificially deactivated, were extensively evaluated in the laboratory using two MAT units of different reactor configuration (SCT-MAT and AUTOMAT). It seems that both units can provide the same ranking of the activity and selectivity of FCC catalysts under study. However, AUTOMAT unit (fluid-bed reactor) proved to be slightly more accurate, when testing catalysts with accessibility differences.

Comparison between the two equilibrium catalysts revealed that E-Cat-HA (highly accessible) is more active because of its ability to crack bigger molecules and its bigger UCS. Furthermore, the HA-Cat manages to get advantage of all its potential activity, before the complete pore plugging during deactivation, in contrast with the LA-Cat sample. In the latter case, there is a number of active sites remaining unexploited, after complete deactivation. The fact that the HA-Cat sample produces more coke and hydrogen can be attributed both to its higher UCS and to the enhanced effect of the contaminant metals due to lower limitation of access to the active sites and pore structure of the catalyst. The higher olefinicities of the HA-Cat sample is an accessibility effect, as the primary produced olefins can diffuse out of the particle before they get involved in secondary hydrogen transfer reactions. Furthermore, its bigger UCS should have promoted the hydrogen transfer reactions due to increment of acid sites density. Instead of promotion, a limitation of these reactions was observed indicating the strong effect of accessibility.

The CDU deactivation method was found to be rather more efficient in simulating the real case than CPS, probably because

the method is more realistic, as it mimics cracking-regeneration cycles of the real case. However, the metal effects are overestimated in both techniques and especially on the CPS samples. In this case the hydrogen yields are exaggerated when testing the samples in SCT-MAT and depreciated when testing the samples in AUTOMAT. The high dispersion of nickel due to wet impregnation technique creates more Ni active sites that perform dehydrogenation reactions. This is the reason for the situation observed during evaluation in SCT-MAT unit. The same Ni active sites can perform secondary hydrogenation reactions, which can explain situation observed during evaluation in the AUTOMAT unit, mainly related with the longer reaction time than that used in the SCT-MAT. The oxidation state of Ni is also important, as CPS ends with a reducing step of catalyst treatment and reduced nickel is known as more deleterious. It is possible that the contaminant metals are more active on the artificially deactivated catalysts because both laboratory deactivation methods cannot simulate their ageing during commercial deactivation. Thus, both methods need improvement especially during evaluation of the high accessibility laboratory-deactivated catalytic samples.

The SEM analysis of the catalysts seems to further support our former conclusions. The deposition profile of nickel over the CPS catalytic samples is totally different from the real case (corresponding E-Cats), especially on the high accessibility catalyst. The Ni–Al mixed phases, observed on the E-Cat samples are probably formed during metal ageing and are less active concerning FCC catalyst deactivation. Absence of such Ni–Al mixed phases on the laboratory-deactivated samples indicates the weakness of both techniques to simulate ageing of the metals during real (commercial) deactivation.

## Acknowledgments

This work was partially funded by the Greek Ministry of Education through the Programme PENED (Action 8.3.1, Project No. 03EΔ859.), the GSRT program AKMON 110 and Albemarle Catalysts Company.

## References

[1] J.E. Otterstedt, S.B. Gevert, S.G. Jaras, P.G. Menon, Appl. Catal. 22 (1986) 159–179.
[2] S.K. Park, H.J. Jeon, K.S. Jung, S.I. Woo, Ind. Eng. Chem. Res. 42 (2003) 736–742.
[3] P. O'Connor, A.C. Pouwels, in: B. Delmon, G.F. Froment (Eds.), Studies in Surface Science and Catalysis Catalyst Deactivation, vol. 88, Elsevier, 1994, pp. 129–144.
[4] R.N. Cimbalo, R.L. Foster, S.J. Wachtel, Oil Gas J. 70 (20) (1972) 112–122.
[5] E.T. Habib, H. Owen, P.W. Synder, C.W. Streed, P. Venuto, Ind. Eng. Chem., Prod. Res. Dev. 16 (4) (1977) 291–296.
[6] B.K. Sporangelo, W.J. Reagan, Oil Gas J. 30 (1984) 139–143.
[7] P.F. Schubert, in: Proceedings of the ACS Symposium on Advances in FCC, N. Orleans, 1997.
[8] J. Sexton, C. Mays, D. Bartholic, R. Abdillah, K. Ambarajava, AIChE Spring Meeting, N. Orleans, 1998.
[9] W. Vreugdenhi, E.T.C. Vogt, R.C. Skocpol, S.J. Yanik, Akzo Nobel Catalysts Symposium, 1998.
[10] J. Scherzerm, J.L. Bass, J. Catal. 28 (1973) 101–105.
[11] S. Moreno, G. Poncelet, Microporous Mater. 12 (1997) 197–222.
[12] P. O'Connor, J.P.J. Verlaan, S.J. Yanik, Catal. Today 43 (1998) 305–313.
[13] P. O'Connor, A.P. Humphries, ACS Preprints 38 (3) (1993) 598.
[14] R.C. Vieira, J.C. Pinto, E.C. Biscaia Jr., C.M.L.A. Baptista, H.C. Cerqueira, Ind. Eng. Chem. Res. 43 (2004) 6027–6034.
[15] T. Boock, T.F. Petti, J.A. Rudesill, International Symposium on Deactivation and Testing of Hydrocarbon Conversion Catalysts Presented before the Division of Petroleum Chemistry, Inc. 210th National Meeting, ACS Chicago, IL, August 20–25, 1995.
[16] D.R. Rainer, E. Rautiainen, P. Imphof, Appl. Catal. A 249 (2003) 69–80.
[17] A.A. Lappas, L. Nalbandian, D.K. Iatridis, S.S. Voutetakis, I.A. Vasalos, Catal. Today 65 (2001) 233–240.
[18] E.S. Kikkinides, A.A. Lappas, A. Nalbandian, I.A. Vasalos, Chem. Eng. Sci. 57 (2002) 1011–1025.
[19] R. Fletcher, A. Hakuli, P. Imhof, Oil Gas J. (2002) 54–59.
[20] D. Wallenstein, R.H. Harding, J.R.D. Nee, L.T. Boock, Appl. Catal. A 204 (2000) 89–106.
[21] R.F. Wormsbecher, A.W. Peters, J.M. Maselli, J. Catal. 100 (1986) 130–137.
[22] A.A. Lappas, D.T. Patiaka, B.D. Dimitriadis, I.A. Vasalos, Appl. Catal. A 152 (1997) 7–26.
[23] E. Rautiainen, P. van Krugten, Akzo Nobel Catal. Courier 40 (2000).
[24] P. Imhof, E. Rautiainen, K.Y. Yung, Akzo Nobel Catal. Courier 48 (2002).
[25] C.A. Trujillo, U.N. Uribe, P.-P. Knops-Gerrits, L.A. Oviedo, P.A. Jacons, J. Catal. 168 (1997) 1–15.
[26] L.A. Pine, J. Catal. 125 (1990) 514–524.
[27] T.F. Petti, D. Tomczak, C.J. Pereira, W. Cheng, Appl. Catal. A 169 (1998) 95–109.
[28] V. Cadet, F. Raatz, J. Lynch, Ch. Marcilly, Appl. Catal. 68 (1991) 263–275.
[29] C.P. Kelkar, M. Xu, R.J. Madon, Ind. Eng. Chem. Res. 42 (2003) 426–433.
[30] C.M. Fraga, in: Proceedings of the Fifth International Symposium on the Advances in FCC 218th ACS Meeting, N. Orleans, 1999.
[31] C. Yin, R. Zhao, C. Liu, Energy Fuels 17 (2003) 1356–1359.
[32] V.B. Kazansky, I.R. Subbotina, F. Jentoft, J. Catal. 240 (2006) 66–72.